# Ring-down waveform extraction by Auto-Regressive approach

**Hisaaki Shinkai**
(Osaka Institute of Technology)
hisaaki.shinkai@oit.ac.jp

## Outline & Summary

The ring-down part of gravitational waves in the final stage of merger of compact objects tells us the nature of strong gravity which can be used for testing the theories of gravity. The ring-down wave, however, fades out in a very short time with a few cycles, and hence it is challenging for gravitational wave data analysis to extract the ringdown frequency and its damping time scale.

We develop a new method, the autoregressive modeling (AR) approach, which extracts waveform by fitting a linear function from bare data. It works well for small number of data points, and does not require any templates. After obtaining the best parameters using mockdata, we applied this method for black-hole merger events of the LIGO/Virgo O1 and O2. We find that for high SNR events, we can extract ring-down waves properly.

This method may work for extracting higher modes of ring-down waves, and implementations are on-going.

## Motivation & O1/O2 data

**Towards testing gravity theories ⇒ Ringdown-part extraction is a key**

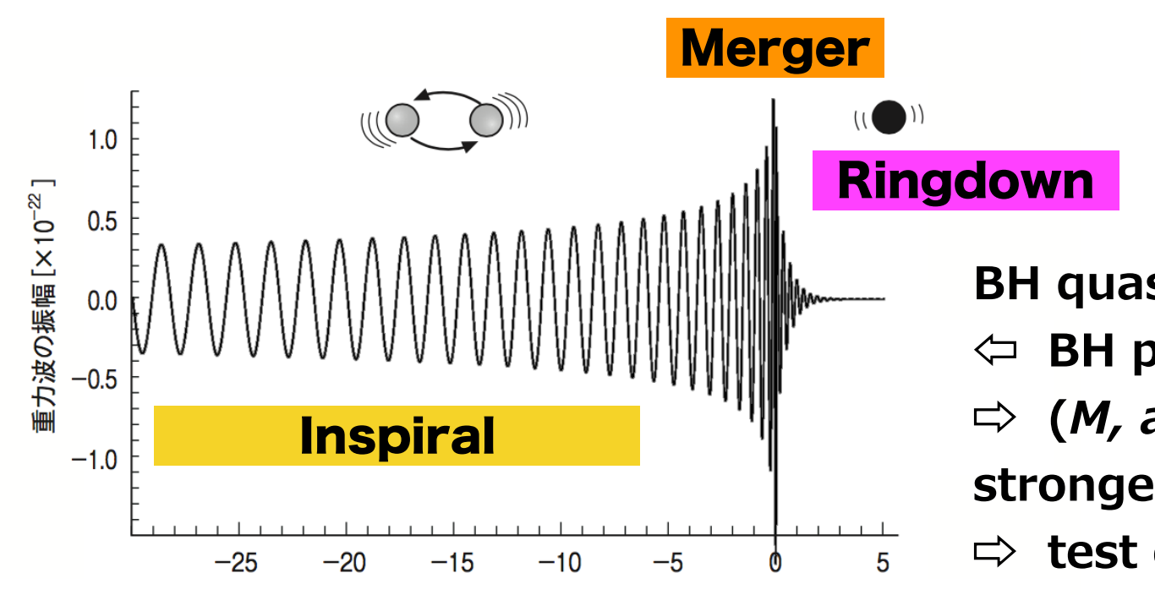

**BH quasi-normal modes**
**⇦ BH perturbation theory**
**⇨ (*M, a*)**
**strongest gravity we can observe**
**⇨ test of gravity theories**

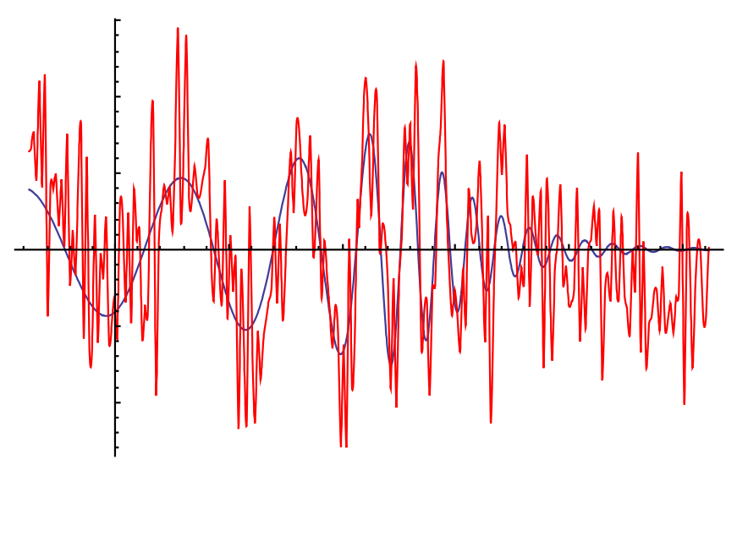

**For *60M* BH of *a*=0.75,**
**frequency = 300 Hz**
**damping time scale = 3.7 ms**

LVC, PRX9 (2019) 031040

**LIGO/Virgo O1/O2 catalogue**

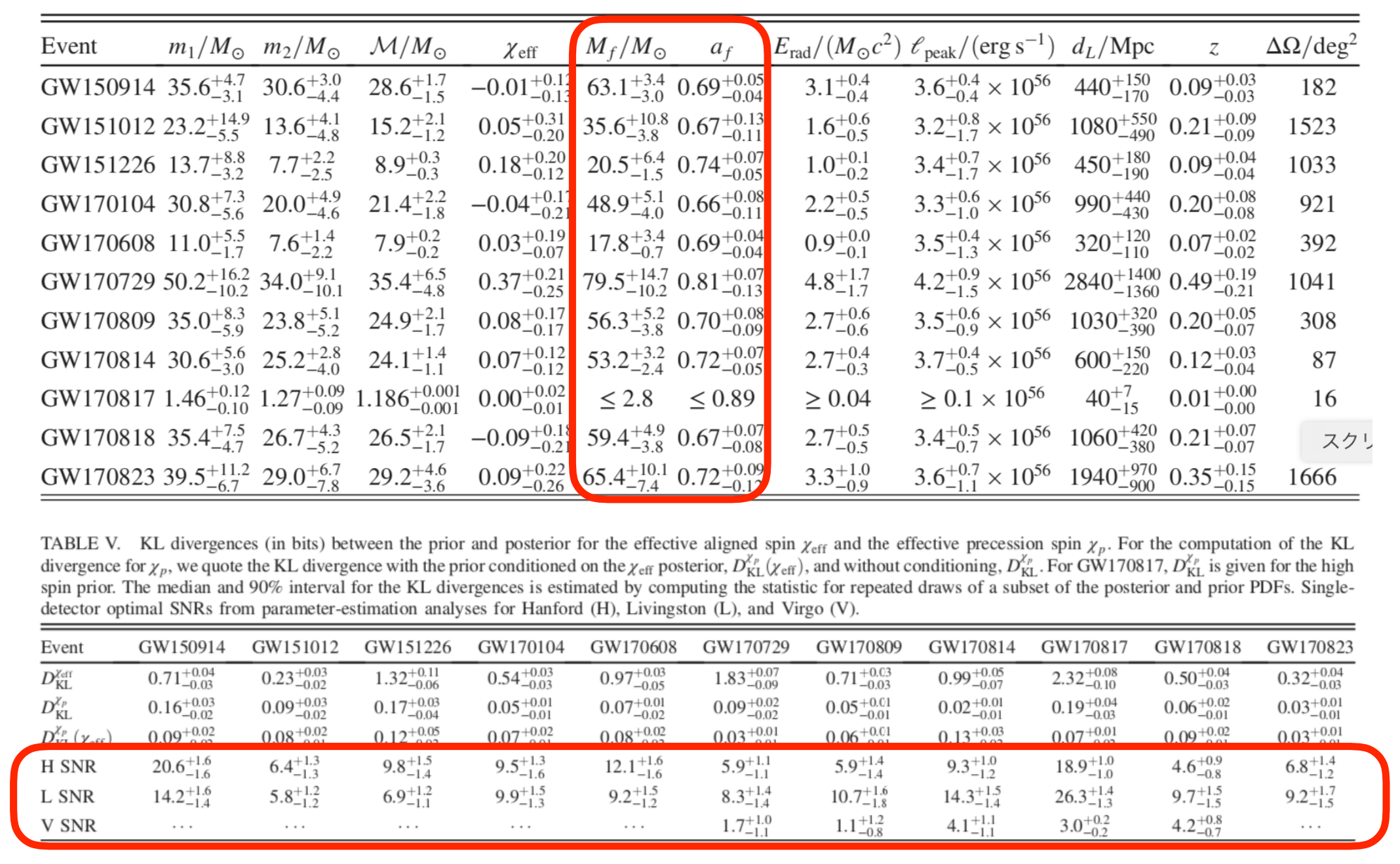

| Event | $m_1/M_\odot$ | $m_2/M_\odot$ | $\mathcal{M}/M_\odot$ | $\chi_{\rm eff}$ | $M_f/M_\odot$ | $a_f$ | $E_{\rm rad}/(M_\odot c^2)$ | $\ell_{\rm peak}/({\rm erg\,s^{-1}})$ | $d_L$/Mpc | $z$ | $\Delta\Omega/{\rm deg}^2$ |
|---|---|---|---|---|---|---|---|---|---|---|---|
| GW150914 | $35.6^{+4.7}_{-3.1}$ | $30.6^{+3.0}_{-4.4}$ | $28.6^{+1.7}_{-1.5}$ | $-0.01^{+0.12}_{-0.13}$ | $63.1^{+3.4}_{-3.0}$ | $0.69^{+0.05}_{-0.04}$ | $3.1^{+0.4}_{-0.4}$ | $3.6^{+0.4}_{-0.4}\times10^{56}$ | $440^{+150}_{-170}$ | $0.09^{+0.03}_{-0.03}$ | 182 |
| GW151012 | $23.2^{+14.9}_{-5.5}$ | $13.6^{+4.1}_{-4.8}$ | $15.2^{+2.1}_{-1.2}$ | $0.05^{+0.31}_{-0.20}$ | $35.6^{+10.8}_{-3.8}$ | $0.67^{+0.13}_{-0.11}$ | $1.6^{+0.6}_{-0.5}$ | $3.2^{+0.8}_{-1.7}\times10^{56}$ | $1080^{+550}_{-490}$ | $0.21^{+0.09}_{-0.09}$ | 1523 |
| GW151226 | $13.7^{+8.8}_{-3.2}$ | $7.7^{+2.2}_{-2.5}$ | $8.9^{+0.3}_{-0.3}$ | $0.18^{+0.20}_{-0.12}$ | $20.5^{+6.4}_{-1.5}$ | $0.74^{+0.07}_{-0.05}$ | $1.0^{+0.1}_{-0.2}$ | $3.4^{+0.7}_{-1.7}\times10^{56}$ | $450^{+180}_{-190}$ | $0.09^{+0.04}_{-0.04}$ | 1033 |
| GW170104 | $30.8^{+7.3}_{-5.6}$ | $20.0^{+4.9}_{-4.6}$ | $21.4^{+2.2}_{-1.8}$ | $-0.04^{+0.17}_{-0.21}$ | $48.9^{+5.1}_{-4.0}$ | $0.66^{+0.08}_{-0.11}$ | $2.2^{+0.5}_{-0.5}$ | $3.3^{+0.6}_{-1.0}\times10^{56}$ | $990^{+440}_{-430}$ | $0.20^{+0.08}_{-0.08}$ | 921 |
| GW170608 | $11.0^{+5.5}_{-1.7}$ | $7.6^{+1.4}_{-2.2}$ | $7.9^{+0.2}_{-0.2}$ | $0.03^{+0.19}_{-0.07}$ | $17.8^{+3.4}_{-0.7}$ | $0.69^{+0.04}_{-0.04}$ | $0.9^{+0.0}_{-0.1}$ | $3.5^{+0.4}_{-1.3}\times10^{56}$ | $320^{+120}_{-110}$ | $0.07^{+0.02}_{-0.02}$ | 392 |
| GW170729 | $50.2^{+16.2}_{-10.2}$ | $34.0^{+9.1}_{-10.1}$ | $35.4^{+6.5}_{-4.8}$ | $0.37^{+0.21}_{-0.25}$ | $79.5^{+14.7}_{-10.2}$ | $0.81^{+0.07}_{-0.13}$ | $4.8^{+1.7}_{-1.7}$ | $4.2^{+0.9}_{-1.5}\times10^{56}$ | $2840^{+1400}_{-1360}$ | $0.49^{+0.19}_{-0.21}$ | 1041 |
| GW170809 | $35.0^{+8.3}_{-5.9}$ | $23.8^{+5.1}_{-5.2}$ | $24.9^{+2.1}_{-1.7}$ | $0.08^{+0.17}_{-0.17}$ | $56.3^{+5.2}_{-3.8}$ | $0.70^{+0.08}_{-0.09}$ | $2.7^{+0.6}_{-0.6}$ | $3.5^{+0.6}_{-0.9}\times10^{56}$ | $1030^{+320}_{-390}$ | $0.20^{+0.05}_{-0.07}$ | 308 |
| GW170814 | $30.6^{+5.6}_{-3.0}$ | $25.2^{+2.8}_{-4.0}$ | $24.1^{+1.4}_{-1.1}$ | $0.07^{+0.12}_{-0.12}$ | $53.2^{+3.2}_{-2.4}$ | $0.72^{+0.07}_{-0.05}$ | $2.7^{+0.4}_{-0.3}$ | $3.7^{+0.4}_{-0.5}\times10^{56}$ | $600^{+150}_{-220}$ | $0.12^{+0.03}_{-0.04}$ | 87 |
| GW170817 | $1.46^{+0.12}_{-0.10}$ | $1.27^{+0.09}_{-0.09}$ | $1.186^{+0.001}_{-0.001}$ | $0.00^{+0.02}_{-0.01}$ | $\le 2.8$ | $\le 0.89$ | $\ge 0.04$ | $\ge 0.1\times10^{56}$ | $40^{+7}_{-15}$ | $0.01^{+0.00}_{-0.00}$ | 16 |
| GW170818 | $35.4^{+7.5}_{-4.7}$ | $26.7^{+4.3}_{-5.2}$ | $26.5^{+2.1}_{-1.7}$ | $-0.09^{+0.18}_{-0.21}$ | $59.4^{+4.9}_{-3.8}$ | $0.67^{+0.07}_{-0.08}$ | $2.7^{+0.5}_{-0.5}$ | $3.4^{+0.5}_{-0.7}\times10^{56}$ | $1060^{+420}_{-380}$ | $0.21^{+0.07}_{-0.07}$ | スクリ |
| GW170823 | $39.5^{+11.2}_{-6.7}$ | $29.0^{+6.7}_{-7.8}$ | $29.2^{+4.6}_{-3.6}$ | $0.09^{+0.22}_{-0.26}$ | $65.4^{+10.1}_{-7.4}$ | $0.72^{+0.09}_{-0.12}$ | $3.3^{+1.0}_{-0.9}$ | $3.6^{+0.7}_{-1.1}\times10^{56}$ | $1940^{+970}_{-900}$ | $0.35^{+0.15}_{-0.15}$ | 1666 |

TABLE V. KL divergences (in bits) between the prior and posterior for the effective aligned spin $\chi_{\rm eff}$ and the effective precession spin $\chi_p$. For the computation of the KL divergence for $\chi_p$, we quote the KL divergence with the prior conditioned on the $\chi_{\rm eff}$ posterior, $D_{\rm KL}^{\chi_p}(\chi_{\rm eff})$, and without conditioning, $D_{\rm KL}^{\chi_p}$. For GW170817, $D_{\rm KL}^{\chi_p}$ is given for the high spin prior. The median and 90% interval for the KL divergences is estimated by computing the statistic for repeated draws of a subset of the posterior and prior PDFs. Single-detector optimal SNRs from parameter-estimation analyses for Hanford (H), Livingston (L), and Virgo (V).

| Event | GW150914 | GW151012 | GW151226 | GW170104 | GW170608 | GW170729 | GW170809 | GW170814 | GW170817 | GW170818 | GW170823 |
|---|---|---|---|---|---|---|---|---|---|---|---|
| $D_{\rm KL}^{\chi_{\rm eff}}$ | $0.71^{+0.04}_{-0.03}$ | $0.23^{+0.03}_{-0.02}$ | $1.32^{+0.11}_{-0.06}$ | $0.54^{+0.03}_{-0.03}$ | $0.97^{+0.03}_{-0.05}$ | $1.83^{+0.07}_{-0.09}$ | $0.71^{+0.03}_{-0.03}$ | $0.99^{+0.05}_{-0.07}$ | $2.32^{+0.08}_{-0.10}$ | $0.50^{+0.04}_{-0.03}$ | $0.32^{+0.04}_{-0.03}$ |
| $D_{\rm KL}^{\chi_p}$ | $0.16^{+0.03}_{-0.02}$ | $0.09^{+0.03}_{-0.02}$ | $0.17^{+0.03}_{-0.04}$ | $0.05^{+0.01}_{-0.01}$ | $0.07^{+0.01}_{-0.02}$ | $0.09^{+0.02}_{-0.02}$ | $0.05^{+0.01}_{-0.01}$ | $0.02^{+0.01}_{-0.01}$ | $0.19^{+0.04}_{-0.03}$ | $0.06^{+0.02}_{-0.01}$ | $0.03^{+0.01}_{-0.01}$ |
| $D_{\rm KL}^{\chi_p}(\chi_{\rm eff})$ | $0.09^{+0.02}$ | $0.08^{+0.02}$ | $0.12^{+0.05}$ | $0.07^{+0.02}$ | $0.08^{+0.02}$ | $0.03^{+0.01}$ | $0.06^{+0.01}$ | $0.13^{+0.03}$ | $0.07^{+0.01}$ | $0.09^{+0.02}$ | $0.03^{+0.01}$ |
| H SNR | $20.6^{+1.6}_{-1.6}$ | $6.4^{+1.3}_{-1.3}$ | $9.8^{+1.5}_{-1.4}$ | $9.5^{+1.3}_{-1.6}$ | $12.1^{+1.6}_{-1.6}$ | $5.9^{+1.1}_{-1.1}$ | $5.9^{+1.4}_{-1.4}$ | $9.3^{+1.0}_{-1.2}$ | $18.9^{+1.0}_{-1.0}$ | $4.6^{+0.9}_{-0.8}$ | $6.8^{+1.4}_{-1.2}$ |
| L SNR | $14.2^{+1.6}_{-1.4}$ | $5.8^{+1.2}_{-1.2}$ | $6.9^{+1.2}_{-1.1}$ | $9.9^{+1.5}_{-1.3}$ | $9.2^{+1.5}_{-1.2}$ | $8.3^{+1.4}_{-1.4}$ | $10.7^{+1.6}_{-1.8}$ | $14.3^{+1.5}_{-1.4}$ | $26.3^{+1.4}_{-1.3}$ | $9.7^{+1.5}_{-1.5}$ | $9.2^{+1.7}_{-1.5}$ |
| V SNR | ⋯ | ⋯ | ⋯ | ⋯ | ⋯ | $1.7^{+1.0}_{-1.1}$ | $1.1^{+1.2}_{-0.8}$ | $4.1^{+1.1}_{-1.1}$ | $3.0^{+0.2}_{-0.2}$ | $4.2^{+0.8}_{-0.7}$ | ⋯ |

## Method

**Auto-Regressive model (idea)**

Fitting data with linear func.

$$x_n = a_1 x_{n-1} + a_2 x_{n-2} + \cdots + a_M x_{n-M} + \varepsilon = \sum_{j=1}^{M} a_j x_{n-j} + \varepsilon$$

e.g. $x_n = Ae^{-rn\Delta t}\cos(\omega n\Delta t)$

$$Z_1 = e^{-(r-j\omega)\Delta t}, \quad Z_2 = e^{-(r+j\omega)\Delta t} \rightarrow x_n = \frac{A}{2}(Z_1^n + Z_2^n) = (Z_1+Z_2)x_{n-1} - Z_1 Z_2 x_{n-2}$$

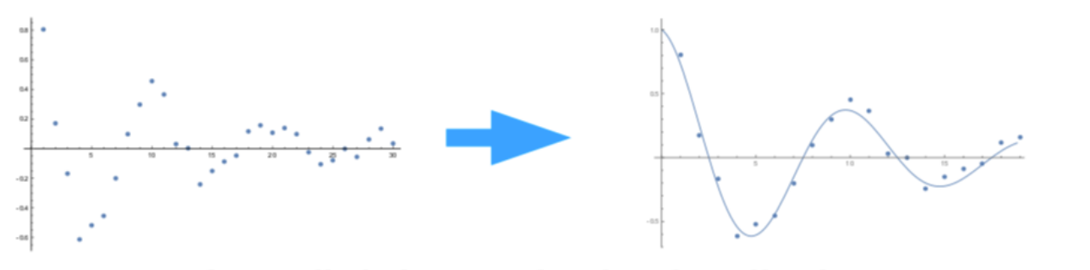

**can be applied also to noisy data by adjusting *M***

**Auto-Regressive model vs Short FFT**

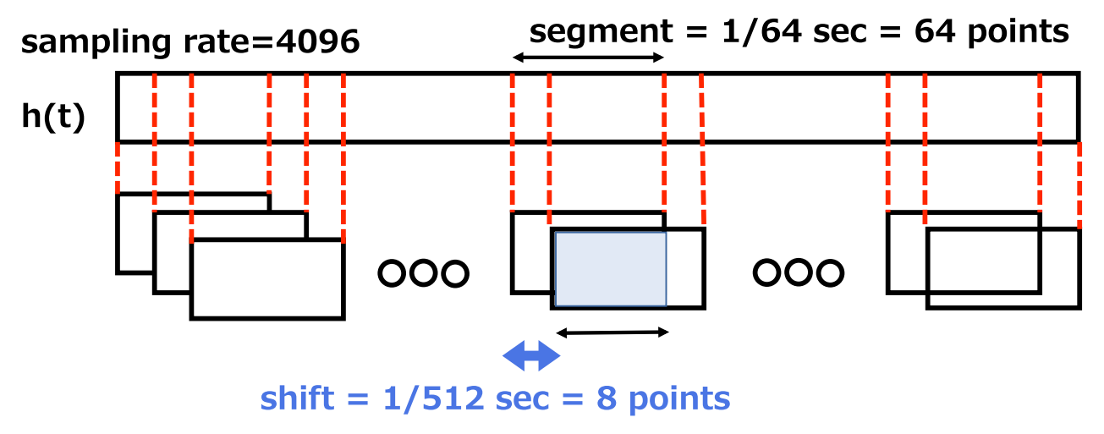

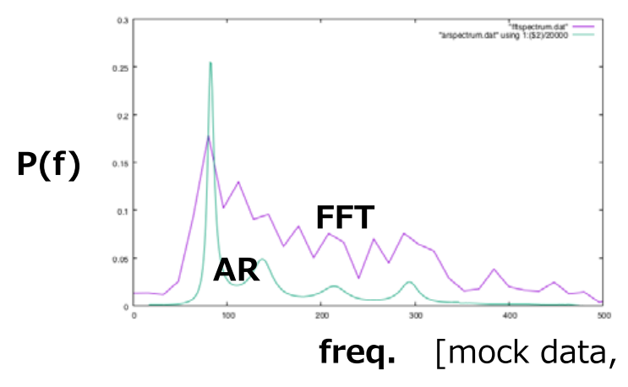

[mock data, SNR=40, inspiral part]

The order *M* can be fixed at 2∼8.

**Even for short segment, AR model shows precise power-spectrum.**

**Auto-Regressive model (Method, general)**

Fitting data with linear func.

$$x_n = a_1 x_{n-1} + a_2 x_{n-2} + \cdots + a_M x_{n-M} + \varepsilon = \sum_{j=1}^{M} a_j x_{n-j} + \varepsilon$$

- find $a_j$ (Burg method)
- find $M$ (FPE final prediction error method)
- re-construct wave signal from fitted function
- apply FFT with arbitrary precision.

power spectrum

$$p(f) = \frac{\sigma^2}{\left|1 - \sum_{j=1}^{M} a_j e^{-I2\pi j f \Delta t}\right|^2}$$

characteristic eq.

$$f(z) = 1 - \sum_{j=1}^{M} a_j z^j = 0$$

$|z_k|$ says amplitude,
$\arg(z_k)$ says frequency.

## Mockdata Comparison

Phys. Rev. D 99, 124032 (2019) [arXiv:1811.06443]

**Mockdata preparation**

**SXS data + shifted ringdown injection + aLIGO noise**

| | |
|---|---|
| modified after t_merger (set A) | 60 set |
| modified before/after t_merger (set B) | 60 set |

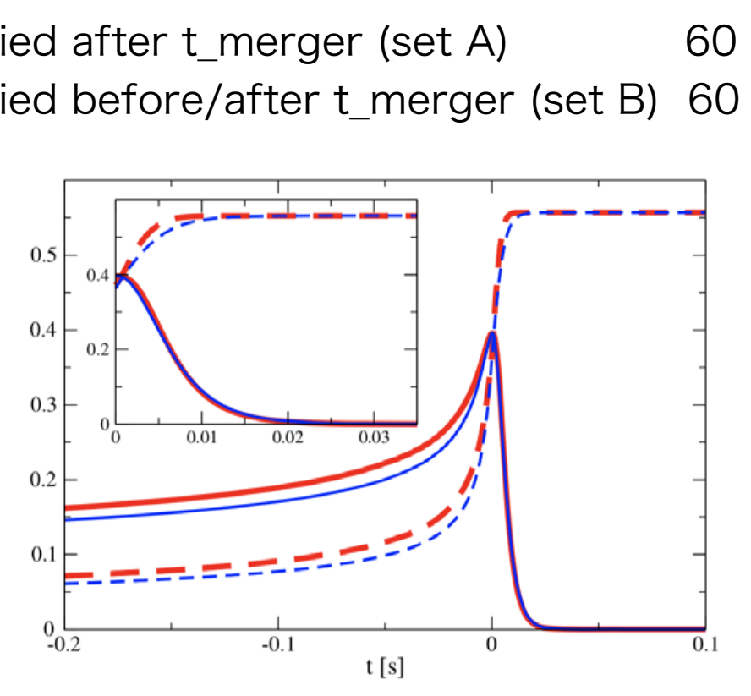

FIG. 1. Examples of sets A and B. (Inset) The ringdown part. Here, set A [(red) thick] with SXS:BBH:0174 and set B [(blue) thin] with SXS:BBH:0002 are shown. The solid lines denote the modified amplitude $A_{22}(t)$, and the dashed lines are the GW frequency $\omega_{22}(t)/(2\pi)$. The total mass is $M = 60M_\odot$, and the real and imaginary parts of the ringdown frequency are 300 and 40 Hz, respectively. The real frequency is obtained by multiplying by 538.609 Hz, and the real amplitude of set A is derived by dividing by 1.37903. The large difference in the inspiral phase is due to the difference of the binary parameters.

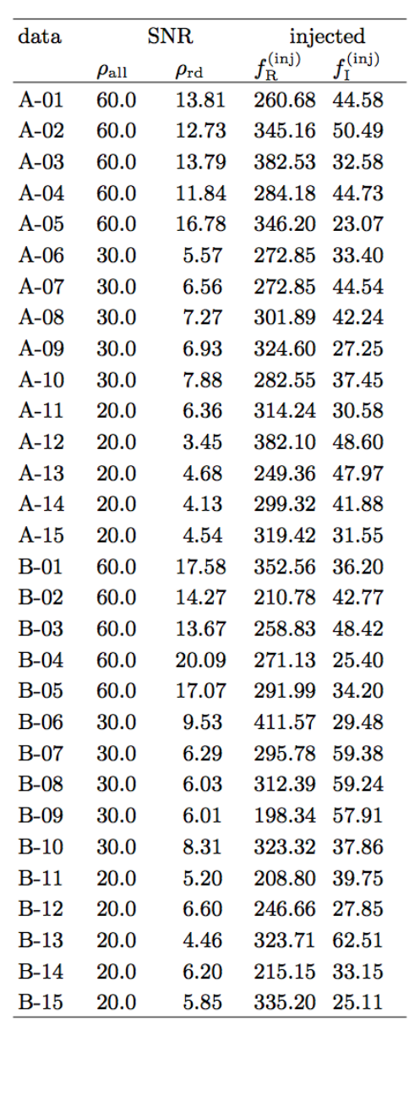

| data | SNR $\rho_{\rm all}$ | SNR $\rho_{\rm rd}$ | injected $f_{\rm R}^{\rm (inj)}$ | injected $f_{\rm I}^{\rm (inj)}$ |
|---|---|---|---|---|
| A-01 | 60.0 | 13.81 | 260.68 | 44.58 |
| A-02 | 60.0 | 12.73 | 345.16 | 50.49 |
| A-03 | 60.0 | 13.79 | 382.53 | 32.58 |
| A-04 | 60.0 | 11.84 | 284.18 | 44.73 |
| A-05 | 60.0 | 16.78 | 346.20 | 23.07 |
| A-06 | 30.0 | 5.57 | 272.85 | 33.40 |
| A-07 | 30.0 | 6.56 | 272.85 | 44.54 |
| A-08 | 30.0 | 7.27 | 301.89 | 42.24 |
| A-09 | 30.0 | 6.93 | 324.60 | 27.25 |
| A-10 | 30.0 | 7.88 | 282.55 | 37.45 |
| A-11 | 20.0 | 6.36 | 314.24 | 30.58 |
| A-12 | 20.0 | 3.45 | 382.10 | 48.60 |
| A-13 | 20.0 | 4.68 | 249.36 | 47.97 |
| A-14 | 20.0 | 4.13 | 299.32 | 41.88 |
| A-15 | 20.0 | 4.54 | 319.42 | 31.55 |
| B-01 | 60.0 | 17.58 | 352.56 | 36.20 |
| B-02 | 60.0 | 14.27 | 210.78 | 42.77 |
| B-03 | 60.0 | 13.67 | 258.83 | 48.42 |
| B-04 | 60.0 | 20.09 | 271.13 | 25.40 |
| B-05 | 60.0 | 17.07 | 291.99 | 34.20 |
| B-06 | 30.0 | 9.53 | 411.57 | 29.48 |
| B-07 | 30.0 | 6.29 | 295.78 | 59.38 |
| B-08 | 30.0 | 6.03 | 312.39 | 59.24 |
| B-09 | 30.0 | 6.01 | 198.34 | 57.91 |
| B-10 | 30.0 | 8.31 | 323.32 | 37.86 |
| B-11 | 20.0 | 5.20 | 208.80 | 39.75 |
| B-12 | 20.0 | 6.60 | 246.66 | 27.85 |
| B-13 | 20.0 | 4.46 | 323.71 | 62.51 |
| B-14 | 20.0 | 6.20 | 215.15 | 33.15 |
| B-15 | 20.0 | 5.85 | 335.20 | 25.11 |

https://gw-genesis.scphys.kyoto-u.ac.jp/ilias/goto_root_fold_669.html
http://www.oit.ac.jp/is/shinkai/mockdatachallenge/

Nakano+, PRD99 (2019) 124032

**mockdata-challenge comparison**

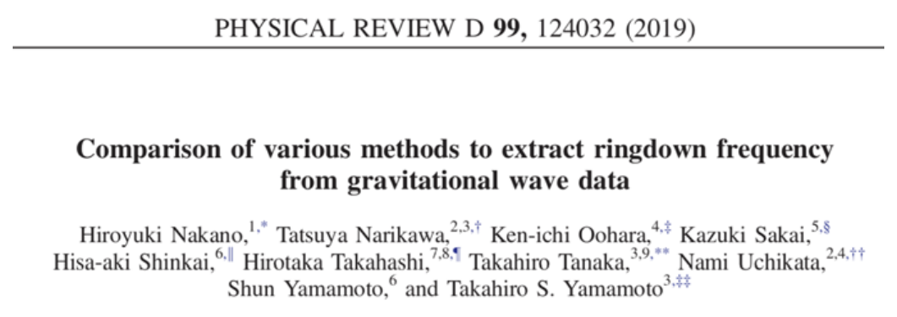

PHYSICAL REVIEW D **99**, 124032 (2019)

**Comparison of various methods to extract ringdown frequency from gravitational wave data**

Hiroyuki Nakano,[1,*] Tatsuya Narikawa,[2,3,†] Ken-ichi Oohara,[4,‡] Kazuki Sakai,[5,§] Hisa-aki Shinkai,[6,∥] Hirotaka Takahashi,[7,8,¶] Takahiro Tanaka,[3,9,**] Nami Uchikata,[2,4,††] Shun Yamamoto,[6] and Takahiro S. Yamamoto[3,‡‡]

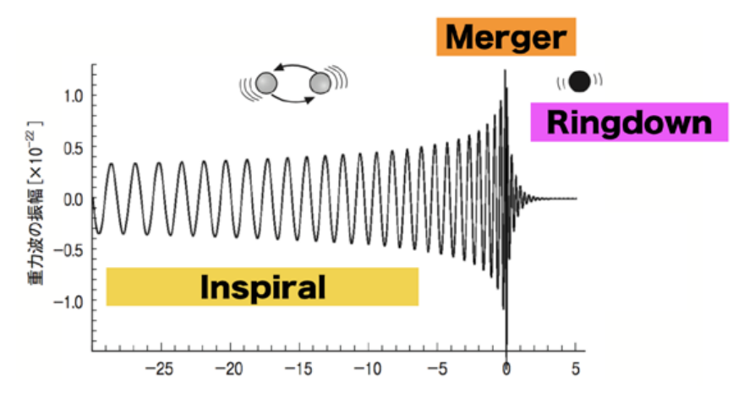

**ringdown search**
**60 mockdata**

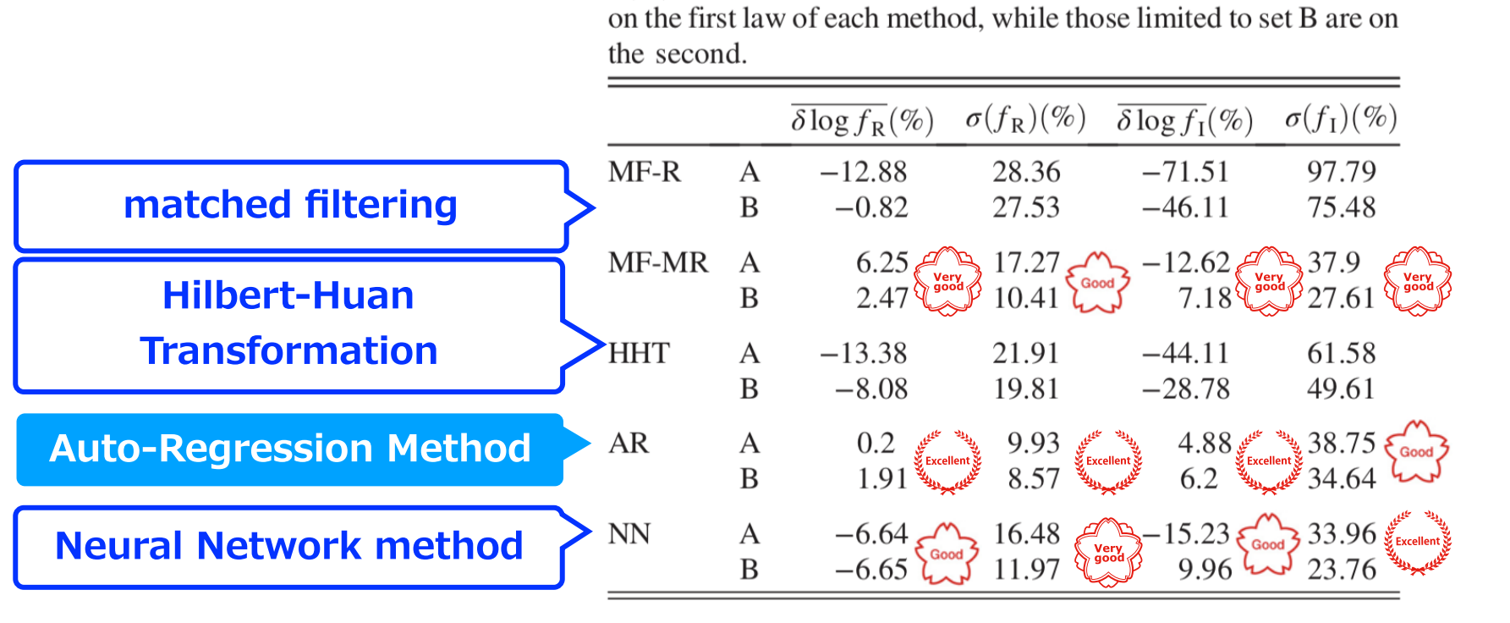

TABLE III. We show the values of $\overline{\delta \log f_{\rm R}}$, $\sigma(f_{\rm R})$, $\overline{\delta \log f_{\rm I}}$, and $\sigma(f_{\rm I})$ for various methods. The results limited to set A are given on the first law of each method, while those limited to set B are on the second.

| | | $\overline{\delta \log f_{\rm R}}$(%) | $\sigma(f_{\rm R})$(%) | $\overline{\delta \log f_{\rm I}}$(%) | $\sigma(f_{\rm I})$(%) |
|---|---|---|---|---|---|
| MF-R | A | −12.88 | 28.36 | −71.51 | 97.79 |
| | B | −0.82 | 27.53 | −46.11 | 75.48 |
| MF-MR | A | 6.25 Very good | 17.27 Good | −12.62 Very good | 37.9 Very good |
| | B | 2.47 | 10.41 | 7.18 | 27.61 |
| HHT | A | −13.38 | 21.91 | −44.11 | 61.58 |
| | B | −8.08 | 19.81 | −28.78 | 49.61 |
| AR | A | 0.2 Excellent | 9.93 Excellent | 4.88 Excellent | 38.75 Good |
| | B | 1.91 | 8.57 | 6.2 | 34.64 |
| NN | A | −6.64 Good | 16.48 Very good | −15.23 Good | 33.96 Excellent |
| | B | −6.65 | 11.97 | 9.96 | 23.76 |

## Results

**GW150914**

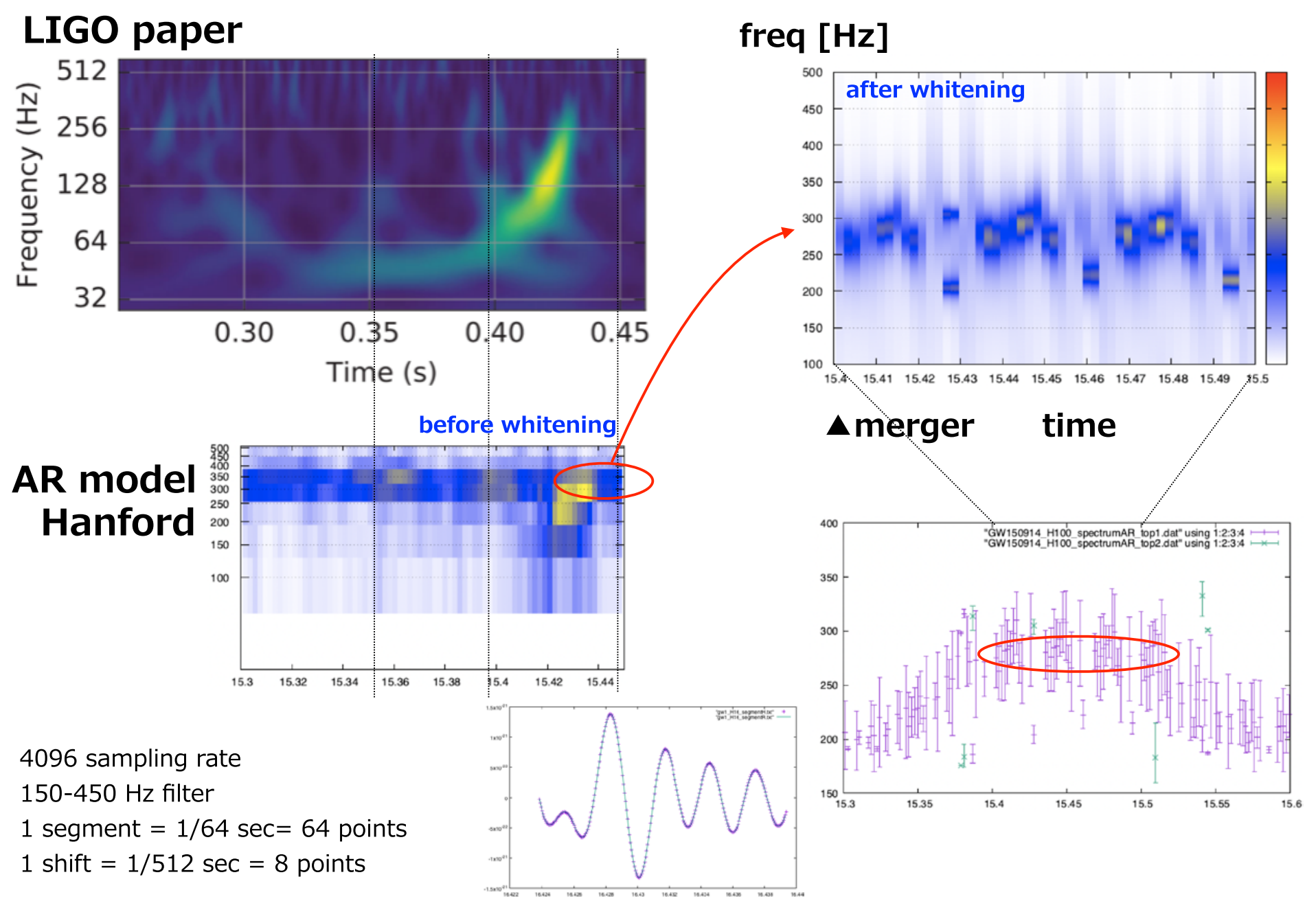

4096 sampling rate
150-450 Hz filter
1 segment = 1/64 sec= 64 points
1 shift = 1/512 sec = 8 points

**GW150914**

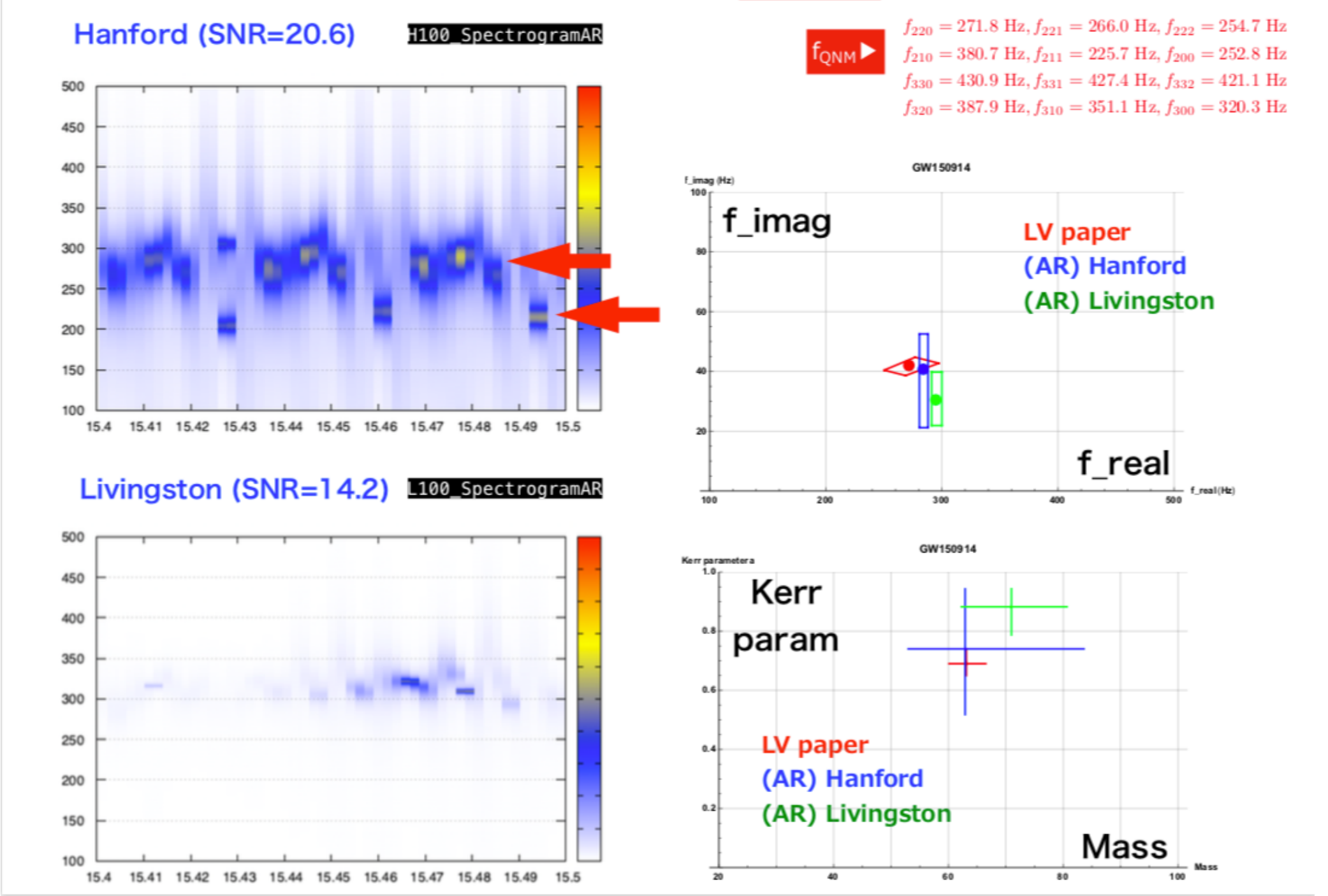

LV paper ▶ $(M,a) = (63.1^{+3.4}_{-3.0}, 0.69^{+0.05}_{-0.04})$

$f_{\rm QNM}$ ▶
$f_{220} = 271.8$ Hz, $f_{221} = 266.0$ Hz, $f_{222} = 254.7$ Hz
$f_{210} = 380.7$ Hz, $f_{211} = 225.7$ Hz, $f_{200} = 252.8$ Hz
$f_{330} = 430.9$ Hz, $f_{331} = 427.4$ Hz, $f_{332} = 421.1$ Hz
$f_{320} = 387.9$ Hz, $f_{310} = 351.1$ Hz, $f_{300} = 320.3$ Hz

**GW170104**

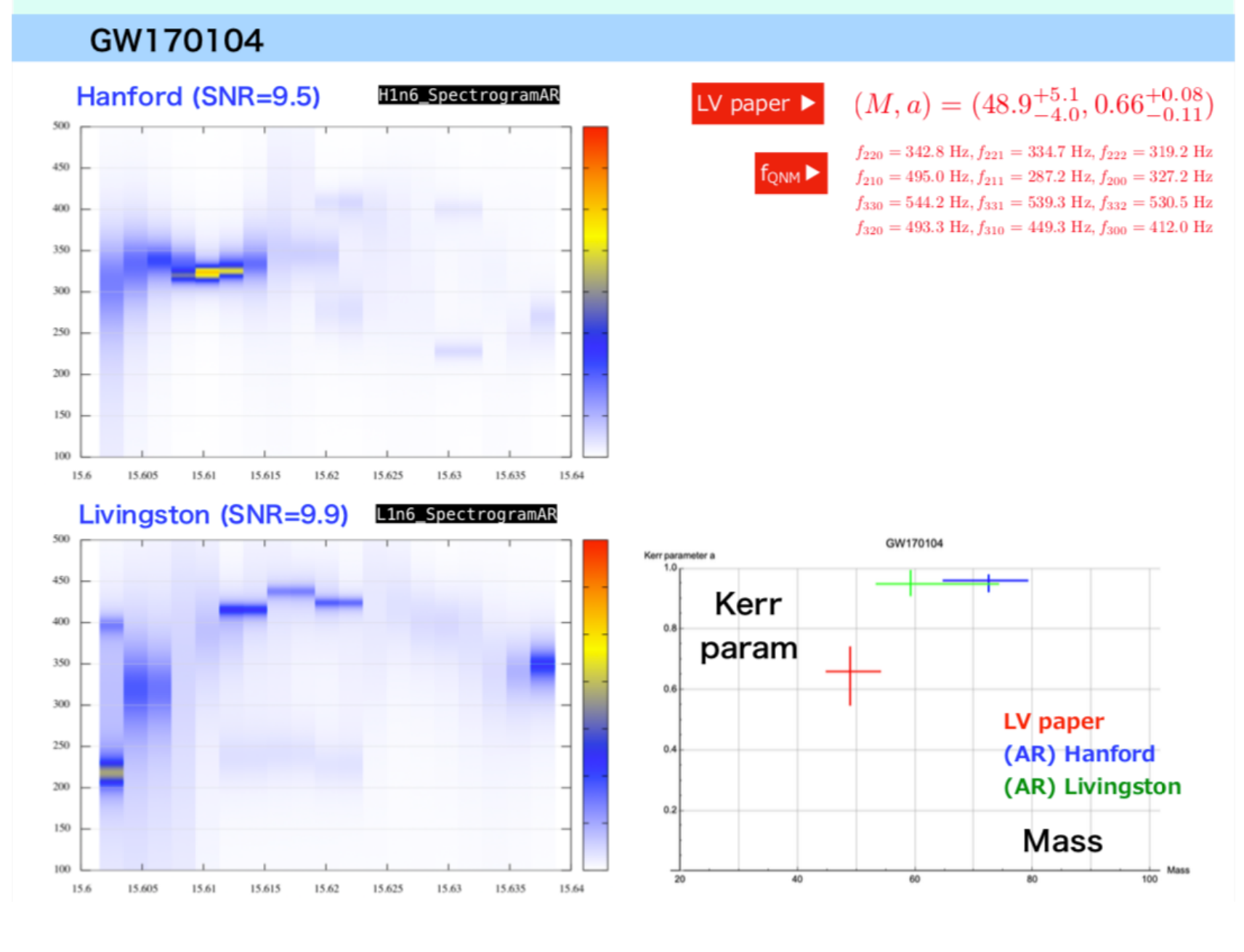

LV paper ▶ $(M,a) = (48.9^{+5.1}_{-4.0}, 0.66^{+0.08}_{-0.11})$

$f_{\rm QNM}$ ▶
$f_{220} = 342.8$ Hz, $f_{221} = 334.7$ Hz, $f_{222} = 319.2$ Hz
$f_{210} = 495.0$ Hz, $f_{211} = 287.2$ Hz, $f_{200} = 327.2$ Hz
$f_{330} = 544.2$ Hz, $f_{331} = 539.3$ Hz, $f_{332} = 530.5$ Hz
$f_{320} = 493.3$ Hz, $f_{310} = 449.3$ Hz, $f_{300} = 412.0$ Hz

**GW170729** $(M,a) = (79.5^{+14.7}_{-10.2}, 0.81^{+0.07}_{-0.13})$

$f_{220} = 240.5$ Hz, $f_{221} = 237.5$ Hz, $f_{222} = 231.3$ Hz
$f_{210} = 291.4$ Hz, $f_{211} = 190.8$ Hz, $f_{200} = 197.6$ Hz

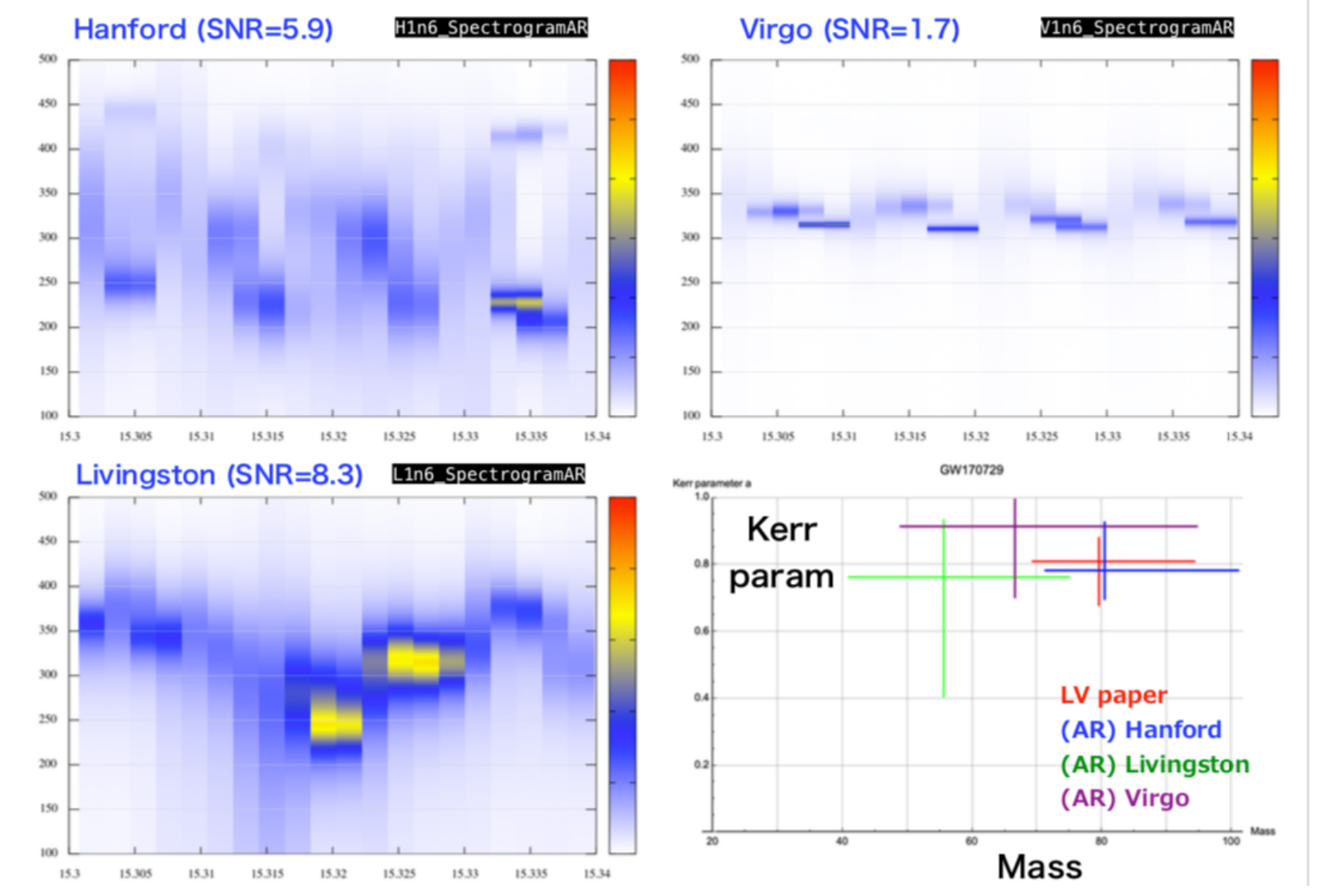

**GW170809** $(M,a) = (56.3^{+5.2}_{-3.8}, 0.7^{+0.08}_{-0.09})$

$f_{220} = 307.0$ Hz, $f_{221} = 300.7$ Hz, $f_{222} = 288.4$ Hz
$f_{210} = 425.6$ Hz, $f_{211} = 254.2$ Hz, $f_{200} = 283.0$ Hz

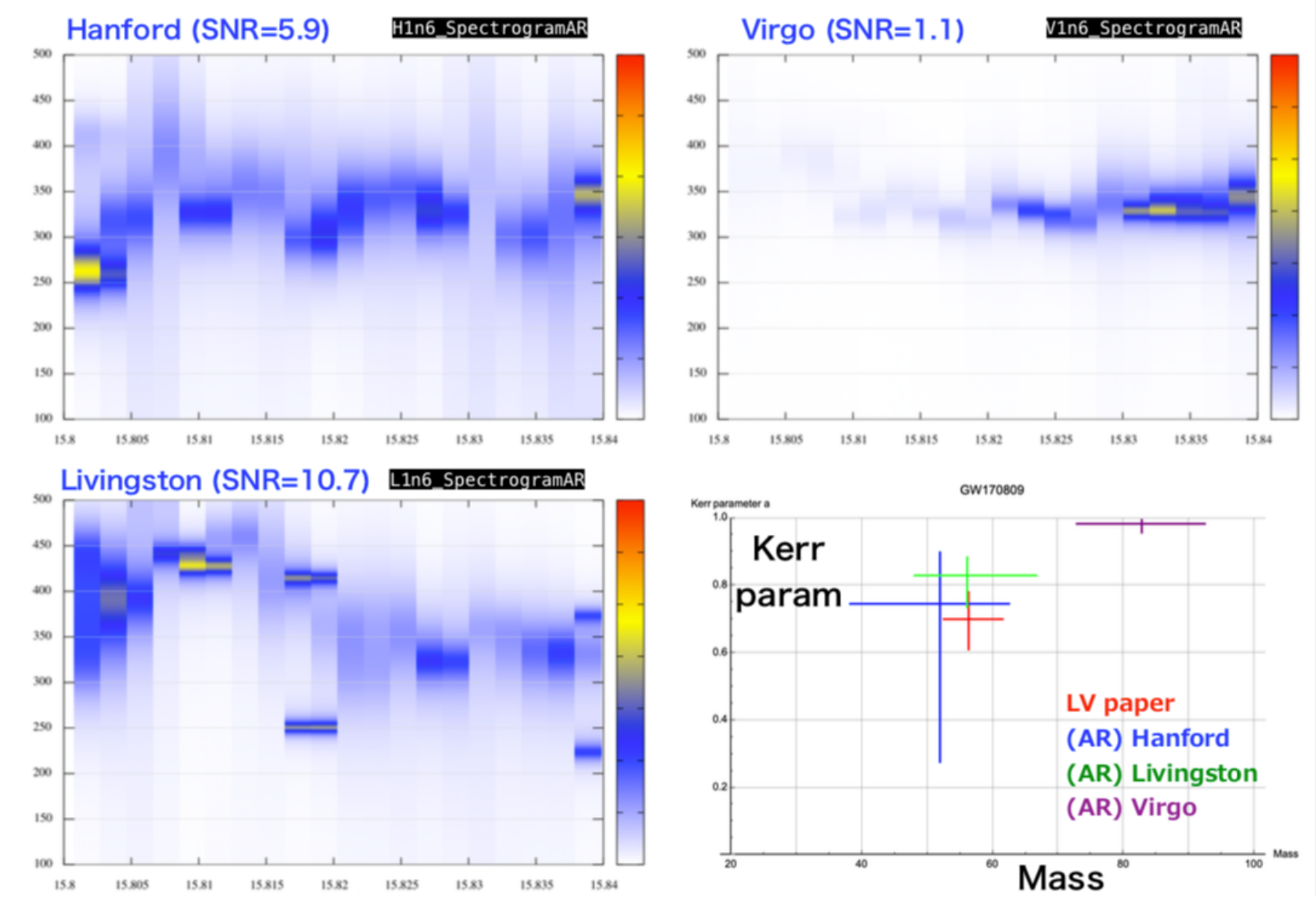

**GW170814** $(M,a) = (53.2^{+3.2}_{-2.4}, 0.72^{+0.07}_{-0.05})$

$f_{220} = 330.3$ Hz, $f_{221} = 324.0$ Hz, $f_{222} = 311.5$ Hz
$f_{210} = 447.9$ Hz, $f_{211} = 271.7$ Hz, $f_{200} = 298.8$ Hz

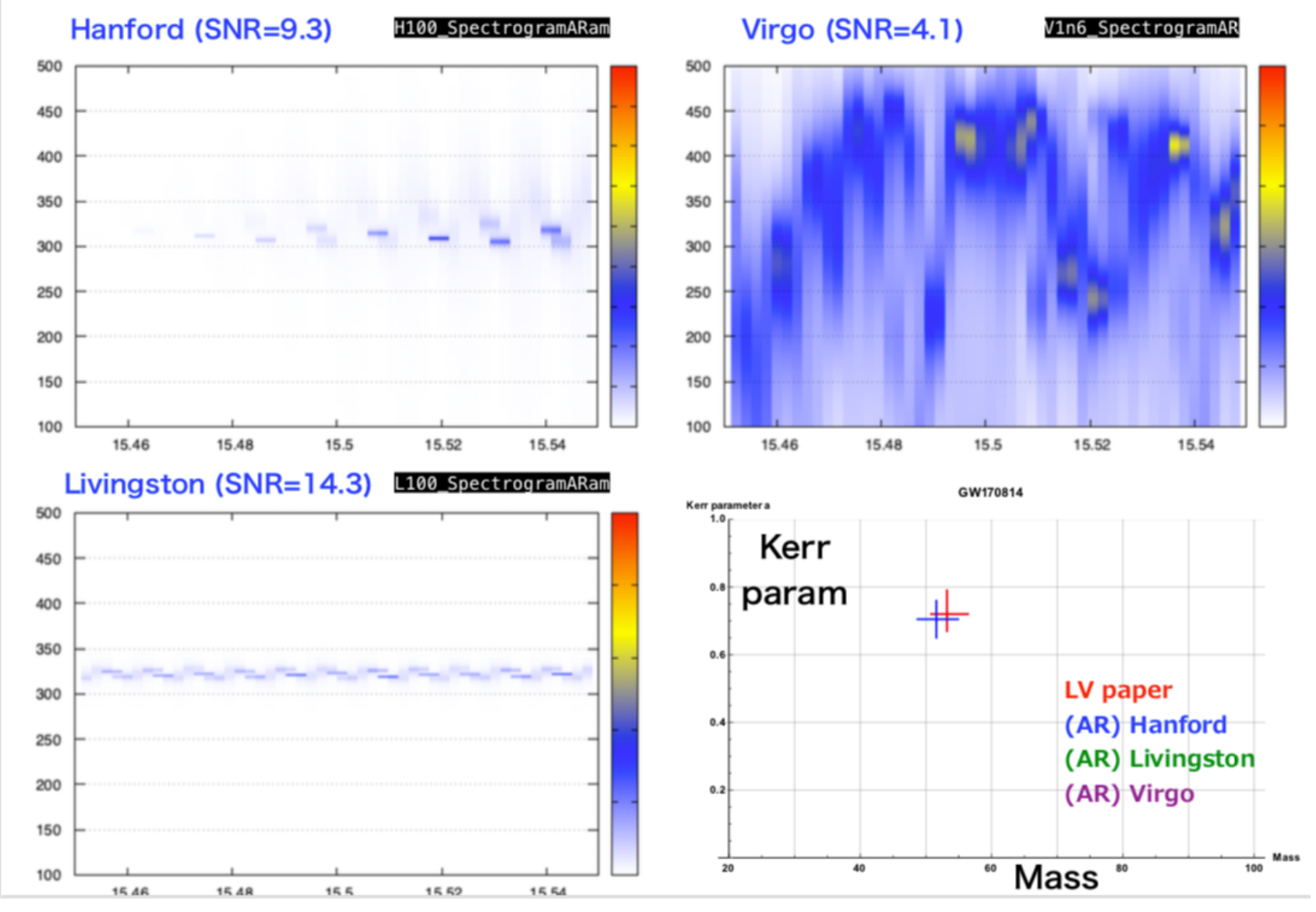

**GW170818** $(M,a) = (59.4^{+4.9}_{-3.8}, 0.67^{+0.07}_{-0.08})$

$f_{220} = 307.0$ Hz, $f_{221} = 300.7$ Hz, $f_{222} = 288.4$ Hz
$f_{210} = 425.6$ Hz, $f_{211} = 254.2$ Hz, $f_{200} = 283.0$ Hz

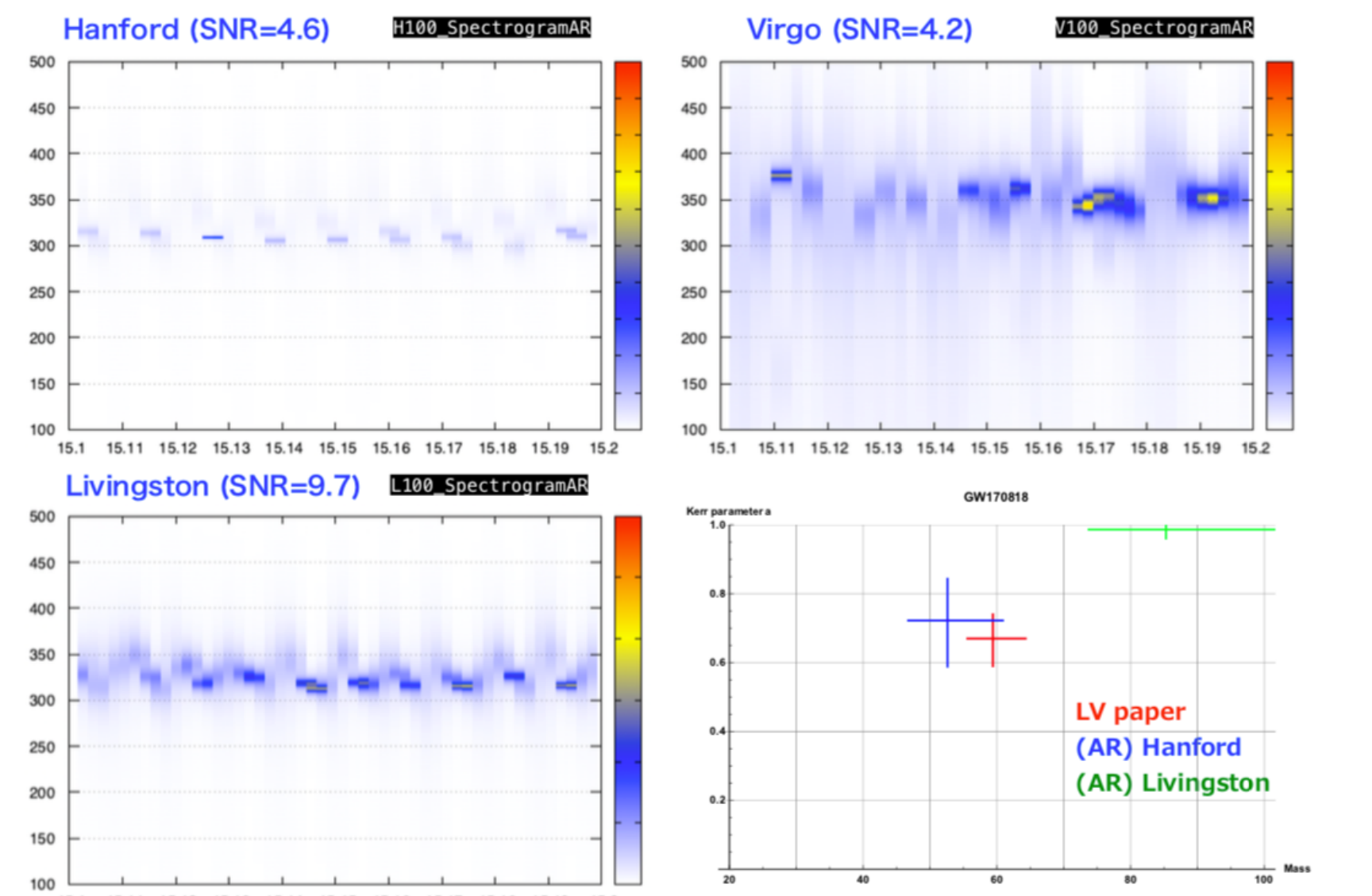

ACKNOWLEDGMENTS

This work was supported by JSPS KAKENHI Grant No. JP17H06358 (and also JP17H06357) [A01: Testing gravity theories using gravitational waves, as a part of the innovative research area, "Gravitational wave physics and astronomy: Genesis"], by JSPS KAKENHI Grant No. JP18K03630 [Non-linear dynamics in the modified gravity theories as a test of string theory] and by No. 19H01901 [New directions in gravitational-wave data analysis: both in computing algorithms and hardwares including its outreach activities].

http://www.oit.ac.jp/is/shinkai/

GWPAW 2019 @ RESCEU, Univ. Tokyo, 2019/10/14-17